

## Anisotropic Constitutive Model for Cracked Reinforced Concrete Element

N. Shirai, T. Sato

*Nihon University, College of Science & Technology, 1-8, Surugadai, Kanda, Chiyoda-ku, Tokyo 101, Japan*

### Abstract

Elasto-plastic behaviors of cracked reinforced concrete are mainly governed by such nonlinear behaviors as 1) compressive responses of concrete between cracks, 2) bond between concrete and reinforcing bars (tension stiffening) and 3) shear transfer effects due to aggregate interlock between cracked concrete surfaces and dowel action of reinforcing bars crossing cracks, and its constitutive law may be formulated on the basis of the theory of anisotropy.

The purposes of this study are first to clarify nonlinear behaviors of cracked reinforced concrete, in particular, the items of 1) and 2), then to derive a suitable analytical model, which can be easily incorporated into an anisotropic constitutive law for smeared type reinforced concrete elements in the finite element applications, and finally to verify the validity of the proposed analytical model.

### 1. Introduction

Constitutive law for cracked reinforced concrete has been often derived by incorporating the stress-strain relationship of concrete cylinder, the tension stiffening of concrete and the shear transfer effects into the theory of anisotropy. However, it is questionable whether the anisotropic constitutive models proposed in the past work satisfactorily in all cases, because of the reasons that 1) principal stress-strain responses induced in cracked concrete are far different from those of concrete cylinder according to the previous test results, 2) in spite of the fact that wall type structures are generally in the combined tensile and compressive stress states, bond and cracking properties of reinforced concrete members under such situation are not fully understood, and 3) it has been experimentally verified that the aggregate interlock and the dowel action are very sensitive to crack widths and spacings, but no reasonable analytical model, which can predict crack widths and spacings correctly, is available. To cope with the first problem, test results on reinforced concrete panels by Collins et al. [1] are rigorously studied, and consequently the principal stress-strain relationship for cracked concrete is approximately expressed in terms of the principal strain ratio. To compensate the second and third problems, bond tests on reinforced concrete prisms subjected to transverse pressures and tensile loads are performed, and the test results such as bond stresses, slips and crack spacings are obtained. Furthermore, a bond-cracking model [2], which can predict not only the tension stiffening of concrete but also crack widths and spacings, is derived on the basis of the bond theory and the test results.

## 2. Anisotropic Constitutive Law for Cracked Reinforced Concrete

It is assumed that the constitutive law for cracked reinforced concrete is expressed in X,Y coordinate system as follows[3].

$$d\{\sigma^{s^0}\}_X = \rho^0 d\{\sigma^0\}_X + \sum_{i=1}^N p_i d\{\sigma^{s^1}\}_X + \rho^0 \sum_{i=1}^N d\{\sigma^{b^1}\}_X + \rho^0 d\{\sigma^a\}_X + \rho^0 \sum_{i=1}^N d\{\sigma^{d^1}\}_X$$

$$= [\rho^0 [D^0]_X + \sum_{i=1}^N p_i [D^{s^1}]_X + \rho^0 \sum_{i=1}^N [D^{b^1}]_X + \rho^0 [D^a]_X + \rho^0 \sum_{i=1}^N [D^{d^1}]_X] d\{\varepsilon^{s^0}\}_X \quad (1.a)$$

in which,

$$[D^0]_X = E \begin{bmatrix} C_{or}^4 & C_{or}^2 C_{or}^2 & C_{or}^3 S_{or} \\ & S_{or}^4 & C_{or} S_{or}^3 \\ \text{SYM.} & & C_{or}^2 S_{or}^2 \end{bmatrix} \quad [D^{b^1}]_X = E \begin{bmatrix} C_1^4 & C_1^2 S_1^2 & C_1^3 S_1 \\ & S_1^4 & C_1 S_1^3 \\ \text{SYM.} & & C_1^2 S_1^2 \end{bmatrix} \quad (1.b, c)$$

$$C_{or} = c \cos \theta_{or}, \quad S_{or} = s \sin \theta_{or}, \quad C_1 = c \cos \theta_1, \quad S_1 = s \sin \theta_1$$

where, the subscript  $i(=1,2,\dots,N)$  indicates the bar direction;  $d\{\sigma^{s^0}\}_X$ ,  $d\{\sigma^0\}_X$  and  $d\{\sigma^{s^1}\}_X$  the stress increments of reinforced concrete, concrete and steel elements;  $d\{\sigma^{b^1}\}_X$ ,  $d\{\sigma^a\}_X$  and  $d\{\sigma^{d^1}\}_X$  the equivalent concrete stress increments due to tension stiffening, aggregate interlock and dowel action;  $[D^0]_X$  and  $[D^{s^1}]_X$  the material stiffnesses of concrete and reinforcements;  $[D^{b^1}]_X$ ,  $[D^a]_X$  and  $[D^{d^1}]_X$  the equivalent material stiffnesses due to tension stiffening, aggregate interlock and dowel action;  $\rho^0$  the concrete density;  $p_i$  the steel ratio;  $E$  the tangent modulus of uniaxial stress-strain curve of concrete;  $E$  the tension stiffness of concrete due to bond;  $\theta_{or}$  the angle between X-axis and the crack direction; and  $\theta_1$  the angle between X-axis and the bar axis. In the present paper, an analytical model for estimating compressive stress-strain responses of cracked concrete and tension stiffening and an approximate formula for predicting crack widths and spacings are developed.

## 3. Stress-Strain Relationship for Cracked Concrete Element

Collins et al. tested orthogonally reinforced concrete panels, which have the size of 89cm x 89cm and the thickness of 7cm, under shear and normal stresses[1]. Figure 1 shows the normalized compressive principal stress,  $|\sigma \dot{\gamma}/f'_c|$  (positive in tension)-strain,  $|\varepsilon \dot{\gamma}/\varepsilon'_c|$  (positive in tension) relationship, where  $\sigma \dot{\gamma}$  and  $\varepsilon \dot{\gamma}$  are the compressive principal stress and strain of cracked concrete, and  $f'_c$  and  $\varepsilon'_c$  are the compressive strength and corresponding strain of concrete cylinder (positive constants). It is seen that the test values show a wide range of scatters and the  $\sigma \dot{\gamma}-\varepsilon \dot{\gamma}$  responses for cracked concrete are far different from those of concrete cylinder (parabolic equation). To express these complex behaviors in a unified manner, the  $\sigma \dot{\gamma}-\varepsilon \dot{\gamma}$  relationship for cracked concrete is idealized into a tri-linear curve as shown in Fig.2, and the stress-strain relationship of each branch line is expressed in terms of the principal strain ratio,  $|\varepsilon \dot{\gamma}/\varepsilon \dot{\gamma}|$ , where  $\varepsilon \dot{\gamma}$  is the principal tensile strain.

(1) Elastic Range; Branch  $\overrightarrow{OA}(\varepsilon \dot{\gamma}_A, \sigma \dot{\gamma}_A)$ ,  $\varepsilon \dot{\gamma}_A \leq \varepsilon \dot{\gamma} \leq 0$ ,  $\sigma \dot{\gamma}_A \leq \sigma \dot{\gamma} \leq 0$

$$\sigma \dot{\gamma} = E \varepsilon \dot{\gamma} \quad (2.a)$$

in which,  $E = 2f'_c/\varepsilon'_c$ ,  $\sigma \dot{\gamma}_A = -2f'_c/3\beta_m$ ,  $\varepsilon \dot{\gamma}_A = -\varepsilon'_c/3\beta_m$

(2) Strain-hardening Range; Branch  $\overrightarrow{AB}(\varepsilon \dot{\gamma}_B - \varepsilon \dot{\gamma}_A, \sigma \dot{\gamma}_B - \sigma \dot{\gamma}_A)$ ,  $\varepsilon \dot{\gamma}_B \leq \varepsilon \dot{\gamma} \leq \varepsilon \dot{\gamma}_A$ ,  $\sigma \dot{\gamma}_B \leq \sigma \dot{\gamma} \leq \sigma \dot{\gamma}_A$

$$(\sigma \dot{\gamma} - \sigma \dot{\gamma}_A)/(\sigma \dot{\gamma}_B - \sigma \dot{\gamma}_A) = (\varepsilon \dot{\gamma} - \varepsilon \dot{\gamma}_A)/(\varepsilon \dot{\gamma}_B - \varepsilon \dot{\gamma}_A) \quad \therefore \sigma \dot{\gamma} = E \lambda (\varepsilon \dot{\gamma} - \varepsilon'_c) \quad (2.b)$$

in which,  $E \lambda = E \varepsilon'_c/(3\beta_m + 1)$ ,  $\sigma \dot{\gamma}_B = -f'_c/\beta_m = \sigma \dot{\gamma}_m$ ,  $\varepsilon \dot{\gamma}_B = -(\beta_m + 1)\varepsilon'_c/2\beta_m$

(3) Strain-softening Range; Branch  $\overrightarrow{BC}(3\varepsilon_c' - \varepsilon_{\beta B}, 0.2f_c' - \sigma_{\beta B})$ ,  $\varepsilon_{\beta c} \leq \varepsilon_f \leq \varepsilon_{\beta B}$ ,  $\sigma_{\beta c} \leq \sigma_f \leq \sigma_{\beta B}$

$$\sigma_f = E_s(\varepsilon_f + 3\varepsilon_c') - 0.2f_c' \quad (2.c)$$

in which,  $E_s = -(1 - 0.2\beta_m)E_s / (5\beta_m - 1)$ ,  $\sigma_{\beta c} = 0.2f_c'$ ,  $\varepsilon_{\beta c} = 3\varepsilon_c'$

where, the parameter  $\beta_m$  means the ratio of  $f_c'$  to the maximum compressive principal stress of cracked concrete,  $\sigma_m^c$ , and this is approximately written as follows.

$$|\sigma_m^c / f_c'| = 1 / \beta_m, \quad \beta_m = 0.85 + 0.27 |\varepsilon_s' / \varepsilon_f| \quad (3)$$

Figures 3 and 4 show the comparison between the test values and the values calculated by eqs. (2.a, b and c). It is seen that there is a clear correlation between the observed and assumed stress-strain curves.

#### 4. Modeling of Bond Action between Concrete and Reinforcing Bars

##### 4.1. Bond Test on Reinforced Concrete Prism under Transverse Pressure

Reinforced concrete prisms were tested under transverse pressures and tensile loads. Figure 5 shows the test setup used in the test, and the brush type bearing plates were used to minimize frictional resistances between the surfaces of specimens and the bearing plates against axial elongations of specimens. Two kinds of specimens were prepared, that is, the effect of transverse pressures, type of bars and steel ratios on crack propagation properties was studied in the series I, and the effect of transverse pressures and type of bars on bond stresses, steel stresses and slips was investigated in the series II.

The series I is consisted of twenty four concrete prisms with the cross section of 10cm x 10cm and the length of 114cm reinforced by a single bar, and the bars used are the deformed bars with the diameters of 13mm and 19mm and the plain round bars with the diameter of 19mm. The series II is consisted of eight reinforced concrete prisms with the cross section of 15cm x 15cm and the length of 64cm, and the bars used are the deformed and plain bars with the diameter of 19mm, as shown in Fig.6. In the series II, the reinforcing bars were grooved along the bar axis on both sides, and strain distributions were measured by strain gauges pasted on the bases of grooves at the interval of 6.25cm. The transverse pressures of different magnitudes were applied such that the ratio,  $\sigma_N / f_c'$  of average compressive stresses due to transverse pressures,  $\sigma_N$  to compressive strength of concrete,  $f_c'$  became to be 0, 25, 50 and 75 percent. The name of specimens is, for instance, referred to as D19-25, where D(P) indicates the deformed(plain) bars, the next number the diameter and the final number  $\sigma_N / f_c'$  (%).

Figure 7 shows the tensile load, P - average strain,  $\varepsilon_{av}$  curve of D13-25, and Fig.8 shows the relation between the final average crack spacings,  $e_{av}$  and the transverse pressures,  $\sigma_N / f_c'$  for D13 specimens. The predicted values by the bond-cracking model to be stated in the next section are also plotted in Figs.7 and 8. Figure 9 shows the normalized bond stress,  $\overline{\tau} (= \tau / \tau_{max})$  - slip,  $\overline{S} (= S / S_{max})$  relationship of D19-25, where  $\tau$  and S indicate the bond stresses and slips, and  $\tau_{max}$  and  $S_{max}$  mean the maximum values of  $\tau$  and corresponding values of S. The predicted values shown in Fig.9 were calculated by the following exponential function[2].

$$\overline{\tau} = e_{\ln} \{ (e-1) \overline{S}^\alpha + 1 \} / \{ (e-1) \overline{S}^\alpha + 1 \} \quad (4)$$

The following conclusions may be drawn from these test results.

- 1) The effect of transverse pressures on the tension stiffening of concrete is significant,

and it depends on the type of bars and the steel ratios.

- 2) The average crack spacings decrease with an increase of average strain, and the higher the transverse pressures, the smaller the average crack spacings in all cases.
- 3) The bond stresses increase up to a certain limit with an increase of transverse pressures.
- 4) The correlation between observed bond stress-slip relations and predicted ones by the exponential function of eq.(4) is relatively good.

#### 4.2. Derivation of Bond-Cracking Model

Consider cracked concrete segments strengthened by reinforcing bars in an arbitrary direction as shown in Fig.10(a). The reinforced concrete portion between cracks is modeled as the assemblage composed of tensile reinforced concrete prisms in the direction of the bar axes as shown in Fig.10(b). First, assume that stress distributions of reinforced concrete prisms subjected to tensile forces and transverse pressures may be derived from the following differential equation for bond (see Fig.11).

$$d^2 S_x / d X^2 = (1 + n p) \psi \tau_x / E^s A^s \quad (5)$$

where,  $S_x$  and  $\tau_x$  indicate the slips and bond stresses along the bar axis,  $\psi$  the perimeter of reinforcing bar,  $n$  the Young's modulus ratio ( $= E^s / E^c$ ),  $p$  the steel ratio ( $= A^s / A^c$ ),  $E^c$  and  $E^s$  the Young's moduli of concrete and reinforcing bar,  $A^c$  and  $A^s$  the sectional areas of concrete prism and reinforcing bar.

If the  $\tau - S$  relationship was given, then each distribution of the slip,  $S_x$ , the bond stress,  $\tau_x$ , the concrete stress,  $\sigma_x^c$  and the steel stress,  $\sigma_x^s$  can be derived from eq.(5). For simplicity, the  $\tau - S$  relationship is approximated into the rigid-plastic as follows.

$$\tau_x = \tau_y \quad (S_x > 0) \quad (6)$$

where,  $\tau_y$  means the yield bond stress and may be determined by equating the area under the line expressed by eq.(4) to that by eq.(6) with  $\alpha=1$  as follows[2].

$$\tau_y = e \tau_{max} / 2(e - 1) \quad (7)$$

where,  $\tau_{max}$  is the maximum bond stress in which the effect of transverse pressure is considered and may be given as follows[4].

$$\text{for deformed bars; } \tau_{max} = \bar{\tau}_{max} \{1 + 2(\bar{\sigma}_{ra}^c / f_c^c)^2\} - 0.05 \bar{\sigma}_{ra}^c \quad (8.a)$$

$$\text{for plain bars ; } \tau_{max} = \bar{\tau}_{max} + 0.36 \bar{\sigma}_{ra}^c \quad (8.b)$$

$$\text{in which, } \bar{\sigma}_{ra}^c = (A - 1) \sigma_N / 2, \quad A = \{(1 - 2\nu^s)G^c + (1 - \nu^c)G^s\} / \{(1 - 2\nu^s)G^c + G^s\}$$

where,  $\tau_{max}$  is the maximum bond stress at which  $\sigma_N$  equals to zero,  $G^c$  and  $G^s$  the elastic shear moduli of concrete and steel,  $\nu^c$  and  $\nu^s$  the Poisson's ratios of concrete and steel, and  $\sigma_N$  the compressive concrete stress acting normal to the bar axis. Letting the tensile force at the cracking point be  $P$ , then  $S_x$ ,  $\sigma_x^s$  and  $\sigma_x^c$  can be derived from eqs.(5) and (6) as follows.

<p>for <math>0 \leq X \leq \ell_d \leq L</math></p> $S_x = \gamma X^2 / 2 - P X / E^s A^s - (\gamma \ell_d^2 / 2 - P \ell_d / E^s A^s) \quad (9.a)$ $\sigma_x^s = P / A^s - E^s \gamma X / (1 + n p) \quad (9.b)$ $\sigma_x^c = p E^s \gamma X / (1 + n p) \quad (9.c)$	<p>for <math>\ell_d \leq X \leq L</math></p> $S_x = 0 \quad (10.a)$ $\sigma_x^s = n p P / (1 + n p) A^s \quad (10.b)$ $\sigma_x^c = P / (1 + n p) A^c \quad (10.c)$
---	---

$$\text{in which, } \ell_d = P / E^s A^s \gamma \quad \gamma = (1 + n p) \psi \tau_y / E^s A^s$$

The stress distributions by eqs.(9) and (10) can be schematically shown in Fig.11. It is

difficult to calculate P directly in the finite element analysis with the smeared type elements, and thus P shall be expressed in terms of the average strain,  $\epsilon_{av}^s$  in the direction of the bar axis from eq.(9.b).

$$\epsilon_{av}^s = \int_0^L (\sigma_x^s / E^s) dx / L, \quad P = E^s A^s \sqrt{2(1+n_p)} \gamma \epsilon_{av}^s L / (1+2n_p) \quad (11)$$

The tensile concrete stress becomes the maximum,  $\sigma_{max}^c$  at  $X=L$ , and  $\sigma_{max}^c$  is given by eqs.(9.c), (10.c) and (11) as.

$$\sigma_{max}^c = p_i E^s \sqrt{2 \gamma_i \epsilon_{av}^s L_i / (1+n_i p_i)(1+2n_i p_i)} \quad (12)$$

where, the subscript  $i(=1,2,\dots,N)$  of each notation indicates the bar direction.

Although  $\sigma_{max}^c$  is calculated for each bar direction, the bar direction is not always perpendicular to crack directions. Therefore, to obtain the maximum tensile stress,  $\overline{\sigma}_{max}^c$  acting perpendicular to cracks,  $\sigma_{max}^c$  in each reinforcing direction must be transformed into the direction parallel to cracks and summed up.

$$\overline{\sigma}_{max}^c = \sum_{i=1}^N \sigma_{max}^c \sin^2 \theta_{cr}^i, \quad \theta_{cr}^i = \theta_{cr} - \theta_i \quad (13)$$

Letting  $f_c'$  be the uniaxial tensile strength of concrete, then crack occurs when the following inequality is satisfied.

$$\beta f_c' \leq \overline{\sigma}_{max}^c, \quad \beta = 1.0 - 0.8 | \sigma_{cr}^c / f_c' | \quad (14)$$

where,  $\beta$  is the reduction factor of tensile concrete strength under tension-compression stress states, and  $\sigma_{cr}^c$  the compressive concrete stress parallel to cracks. Assumed that crack spacing becomes the minimum,  $e_{min}$  when the equality of eq.(14) holds,  $e_{min}$  can be derived by substituting  $L_i = e_{min} / 2 | \sin \theta_{cr}^i |$  into eqs.(12), (13) and (14) as follows.

$$e_{min} = \left\{ \beta f_c' / \sum_{i=1}^N \left\{ p_i E^s \sqrt{2 \gamma_i \epsilon_{av}^s | \sin^3 \theta_{cr}^i | / (1+n_i p_i)(1+2n_i p_i)} \right\} \right\}^2 \quad (15)$$

It must be needed to evaluate the upper bound of crack spacings, that is, the maximum crack spacing,  $e_{max}$ , on the basis of the energy criteria proposed by Bazant et al.[5].

For simplicity,  $e_{av}$  and crack width,  $W_{av}$  are calculated by assuming that  $e_{max} = k e_{min}$ .

$$e_{av} = (e_{max} + e_{min}) / 2 = (1+k) e_{min} / 2, \quad W_{av} = \epsilon_v e_{av} \quad (16.a, b)$$

where,  $\epsilon_v$  is the average strain normal to cracks and  $k$  is assumed to be equal to 2 in this study. The average concrete stress,  $\sigma_{av}^c$  in each bar direction due to the tension stiffening is derived as follows.

$$\sigma_{av}^c = \{ E^s A^s \gamma_i \lambda_{d1}^2 + 2P_i (L_i - \lambda_{d1}) \} / 2(1+n_i p_i) A_f L_i \quad (17)$$

The authors shall refer to this as the bond-cracking model thereafter.

## 5. Numerical Examples

### 5.1. Analysis of Reinforced Concrete Panels

To verify the validity of the proposed stress-strain relationship for cracked concrete, the finite element analysis was performed on the reinforced concrete panels tested by Collins et al.[1]. The specimens analyzed are PV4 and PV25, and they were tested under the pure shear stress,  $\tau_{xy}$  and the combined stresses of shear stress,  $\tau_{xy}$  and compressive normal stress,

$\sigma_x = \sigma_y = -0.69 \tau_{xy}$ , respectively. Figures 12 and 13 show the shear stress,  $\tau_{xy}$ -shear strain,  $\tau_{xy}$  responses. The values calculated by using the stress-strain relationship of concrete cylinder, that is,  $\beta_n = 1$ , are also plotted in the figures. In the case of PV4, which failed in the steel yielding, both of the calculated values fairly agree with the test

results, and thus  $\beta_m$  has little influence on the shear behaviors.

In the case of PV25, on the other hand, the calculated values taking  $\beta_m$  into account tend to agree with the test results. But, the values calculated by setting  $\beta_m = 1$  give the lower maximum strength than that of the test and show the failure mode of steel yielding, and this failure mode is different from that observed in the test, that is, the shear failure of concrete.

## 5.2. Analysis of Reinforced Concrete Shear Wall

To verify the validity of the bond-cracking model, the finite element analysis was carried out on the reinforced concrete shear wall specimen of one bay and three stories (77W202) subjected to a constant vertical load,  $N (=13.5 \text{ tons})$  and increasing horizontal loads,  $P$  [6]. Figure 14 shows the relation between the horizontal loads,  $P$  and the horizontal displacements,  $\delta$  at the top. Figure 15 shows the comparison between the average crack spacings of the test and the calculated maximum and minimum crack spacings in the wall panel at the first story. Figure 16 shows the comparison between the measured crack widths and the calculated ones in the wall panel at the first story. It seems that the agreement of the test and calculated results is fairly good in every case.

## 6. Conclusions

The effect of the assumed stress-strain relationship of cracked concrete on the shear behaviors is very significant, especially in case of reinforced concrete panels failing in shear. Therefore, it must be needed to assume the stress-strain relationship of cracked concrete carefully, and this relation can be expressed in terms of the principal strain ratio.

The effect of the transverse pressure on bond and cracking properties of reinforced concrete members is remarkable, and the proposed bond-cracking model taking the effect of transverse pressures into account can predict the tension stiffening and the crack widths and spacings accurately.

## References

- [1] VECCHIO, F., COLLINS, M.P., "The Response of Reinforced Concrete to In-Plane Shear and Normal Stresses," Publication No.82-03, University of Toronto, March 1982.
- [2] SHIRAI, N., SATO, T., "Bond-Cracking Model for Reinforced Concrete," Trans. of the Japan Concrete Institute, Vol.6, 1985(to be published).
- [3] SHIRAI, N., SATO, T., "Inelastic Analysis of Reinforced Concrete Shear Wall Structures," IABSE Colloquium, Delft, June 1981, pp.197-210, 687-700.
- [4] SATO, T., SHIRAI, N. et al., "Cracking and Bond Behaviors of Reinforced Concrete Tensile Members under Lateral Pressure," Trans. of the Japan Concrete Institute, Vol.4, 1982, pp.341-348.
- [5] BAZANT, Z.P., OH, B.H., "Spacing of Cracks in Reinforced Concrete," Proc. of the ASCE, Vol.109, No.ST9, Sept. 1983, pp.2066-2085.
- [6] SATO, T., SHIRAI, N. et al., "Experimental Study on Elasto-Plastic Behavior of Reinforced Concrete Shear Wall Structures," Journal of the Research Institute of Science & Technology, Nihon University, No.53, July 1980, pp.1-43.

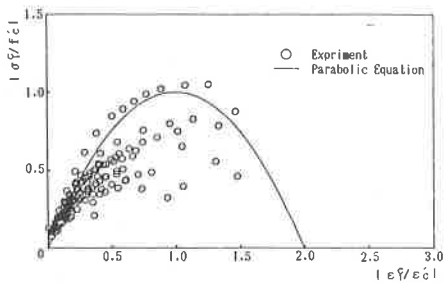


Fig. 1 Compressive Principal Stress-Strain Relationship of Cracked Concrete

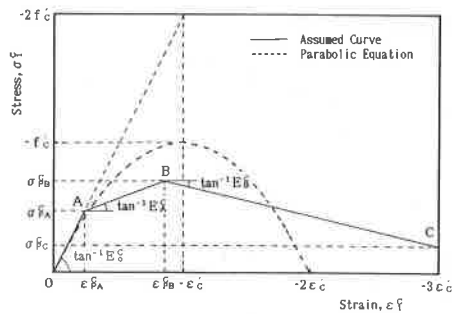


Fig. 2 Assumed Principal Stress-Strain Curve of Cracked Concrete

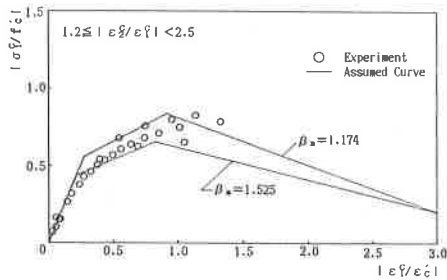


Fig. 3 Principal Stress-Strain Relationship of Cracked Concrete

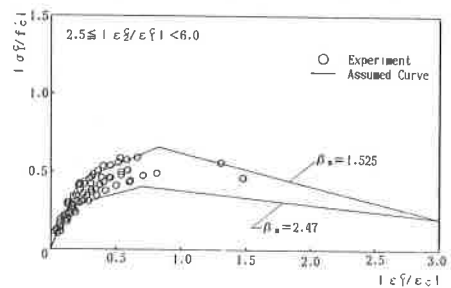


Fig. 4 Principal Stress-Strain Relationship of Cracked Concrete

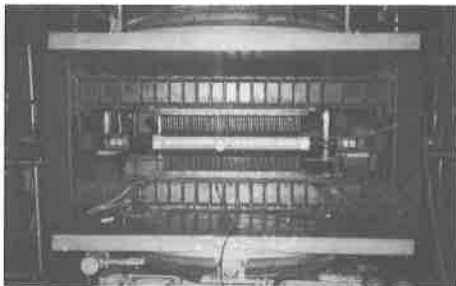


Fig. 5 Loading Setup

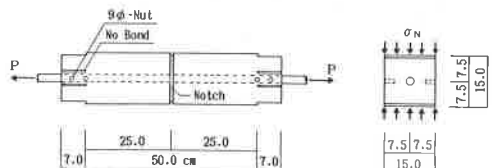


Fig. 6 Tensile Bond Specimen

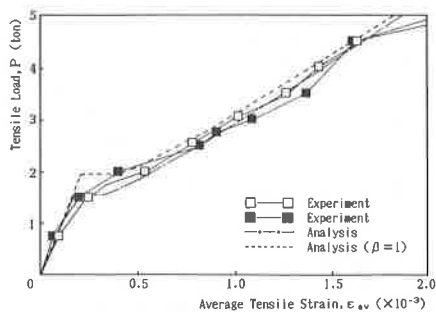


Fig. 7 Tensile Load-Average Strain Relationship

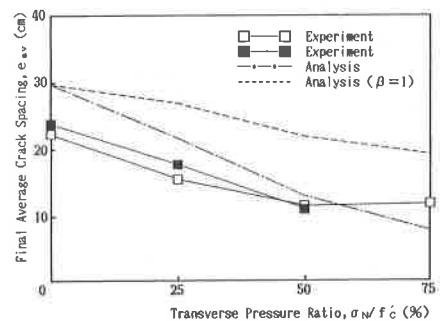


Fig. 8 Final Average Crack Spacing-Transverse Pressure Relationship

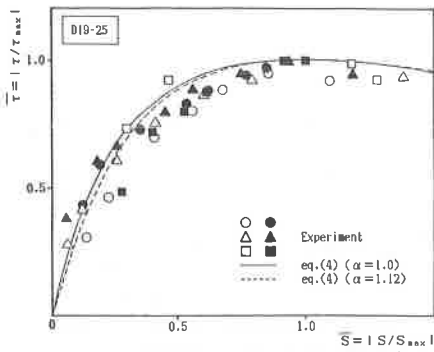


Fig. 9 Normalized Bond Stress-Slip Relationship

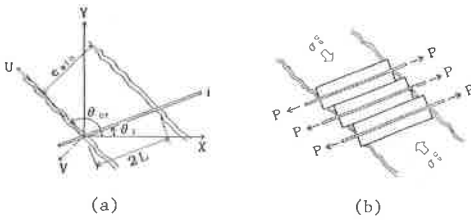


Fig. 10 Modeling of Cracked Reinforced Concrete Segment

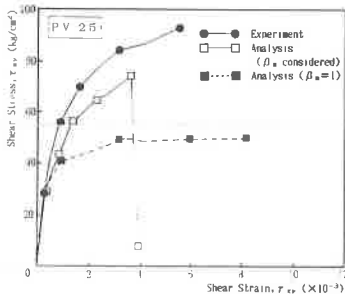


Fig. 13 Shear Stress-Shear Strain Relationship

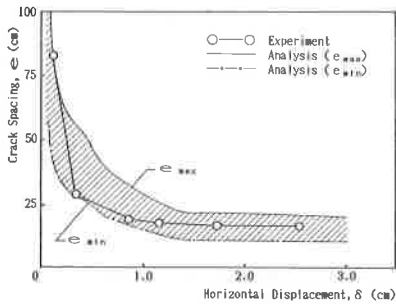


Fig. 15 Crack Spacing-Horizontal Displacement Relationship

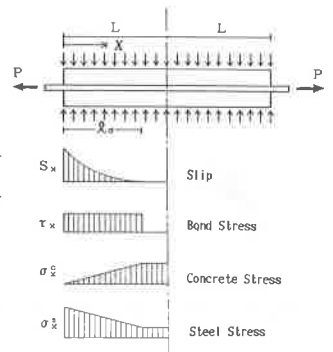


Fig. 11 Stress Distributions of Tensile Member

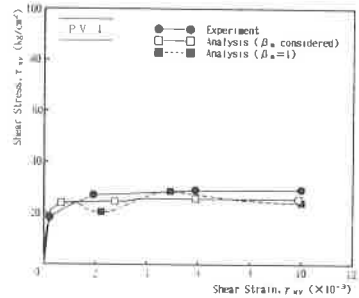


Fig. 12 Shear Stress-Shear Strain Relationship

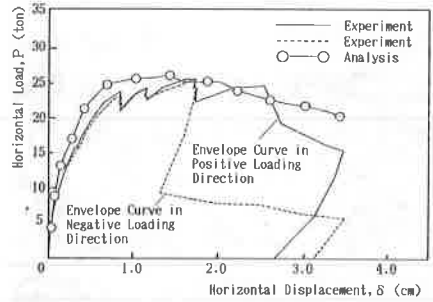


Fig. 14 Horizontal Load-Displacement Relationship

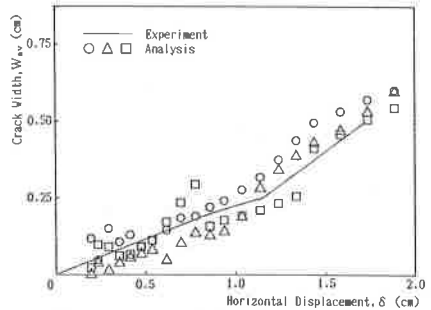


Fig. 16 Crack Width-Horizontal Displacement Relationship